

Effect of intense plastic straining on microstructure and mechanical properties of an Al-Mg-Sc alloy

R. Kaibyshev , E. Avtokratova , O. Sitdikov

Abstract. An Al-5%Mg-0.18%Mn-0.2%Sc-0.08%Zr-0.002%Be was subjected to equal-channel angular extrusion up to true strains of ~ 3 and ~ 8 , that resulted in the formation of partially recrystallized and fully recrystallized structure, respectively. It was shown that the alloy with partially recrystallized structure exhibits highest strength and ductility. The material with fully recrystallized structure showed lowest fatigue crack growth rate and highest value of fracture toughness. Reasons of this unusual effect of microstructure on crack propagation resistance under fatigue are discussed.

1. Introduction

The formation of micron scale grained structure in Al-Mg-Sc alloys by equal-channel angular extrusion (ECAE) technique leads to significant increase in their strength [1] and extraordinary superplastic ductilities [2]. These properties, however, are not sufficient for structural aluminum alloys. For commercial use as a material for critical components of an aircraft the knowledge of fatigue properties and fracture toughness of these alloys processed by ECAE is very important. Unfortunately, the limited number of studies were dealt with examination of these properties in Al-Mg-Sc alloys [3-6]. The aim of the present work is to report effect of ECAE on strength, ductility, fatigue crack growth rate and fracture toughness. It is known [1] that it is possible to produce different microstructure by ECAE varying strain. In this study the mechanical properties were examined for an Al-Mg-Sc alloy with partially recrystallized structure and fully recrystallized structure produced by ECAE.

2. Experimental

The 1570C Al with a chemical composition of Al-5%Mg-0.18%Mn-0.2%Sc-0.08%Zr-0.002%Be (in weight %) was used as the starting material [7]. The ingot was cut into plates with dimensions of 152x152x25 mm³. These plates were subjected to ECAE with rectangular shape of channels up to true strains of ~ 3 and ~ 8 by route B_{cz} at a temperature of 325°C. Details of this ECAE procedure were described in previous works [3,4]. Tensile specimens of 6 mm gauge length and 1.4 x 3 mm² cross-section were machined from these plates with tension axis lying parallel to direction of last extrusion. These samples were tensioned to failure at ambient temperature and a strain rate of $5.6 \times 10^{-3} \text{ s}^{-1}$ using an Instron 1185 testing machine. The tests for cyclic crack resistance were conducted using a Schenk hydropulse PSA hydraulic machine. Compact tension (CT) specimens 20 mm thick were cut in accordance with ASTM Standard E399-06. The specimens were loaded using a sinusoidal cycle with a

frequency of 5 Hz and an asymmetry coefficient $R = 0.1$. The fatigue crack growth rate as a function of the stress-intensity factor range, ΔK , was obtained in accordance with ASTM standard E647-08. Examinations of microstructure and fractured surface were carried out using optical microscope Nikon L-150 and scanning electron microscope JSM-840 equipped with EBSD attachment. Details of structural characterizations were reported previously [3,4,7].

3. Results and discussion

No coarse second-phase particles with a size higher than $1\mu\text{m}$ were found in initial structure [7]. Coherent dispersoids of $\text{Al}_3(\text{Sc,Zr})$ -phase having equiaxed shape and a size ranging from 5 to 10 nm are uniformly distributed within the grains [7]. ECAE up to true strains of ~ 3 and ~ 8 resulted in the formation of partially (fig.1a) and fully (fig.1b) recrystallized structure. Fraction of recrystallized grains is 0.25 and 0.95; their average size is $\sim 1.6\mu\text{m}$ and $\sim 1.2\mu\text{m}$, respectively. Highly elongated unrecrystallized grains aligned along the last extrusion direction can be clearly distinguished in the samples strained up to $\varepsilon\sim 3$ (fig.1a). Careful inspection of Fig.1a shows that subgrains locate within deformation bands.

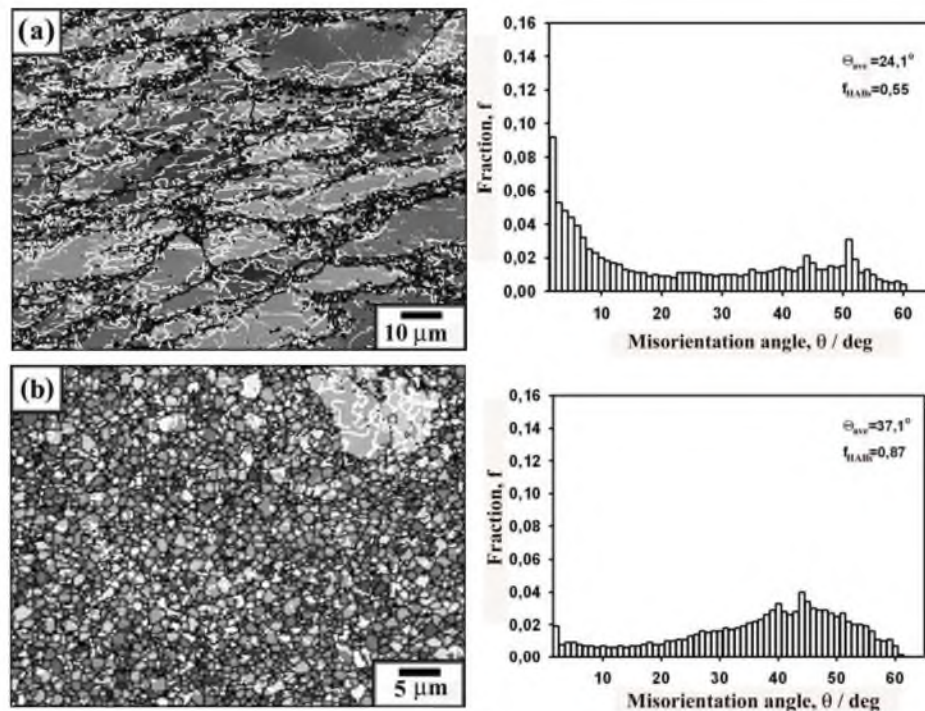


Figure 1. Microstructures in the 1570C after ECAE to a total strain of ~ 3 (a) and ~ 8 (b).

Mechanical properties of the 1570C alloy in initial state and after ECAE with different strains are summarized in Table 1. It is seen that intense plastic straining leads to a significant increase in yield stress; total elongation remains virtually unchanged. Ultimate stress increment is minor. Samples strained to $\varepsilon\sim 3$ exhibit highest strength and ductility. Therefore, the formation of partially recrystallized structure in the 1570C provides highest strength that can be attributed to highest density of lattice dislocations.

In contrast the recrystallized state of the 1570C alloy showed lowest values of fatigue crack growth rate (Fig.2). At stage I, the fatigue crack growth rate for the 1570C alloy with partially recrystallized structure is higher by a factor of 3.75 than that for the alloy with fully recrystallized structure. At

$\Delta K=6 \text{ MPa}\cdot\sqrt{\text{m}}$, fatigue crack propagation growth rates are 3×10^{-8} and 8×10^{-9} m/cycle, respectively. At stage II and $\Delta K=30 \text{ MPa}\cdot\sqrt{\text{m}}$, the values of fatigue crack growth rates are 5.8×10^{-6} and 3.4×10^{-6} m/cycle for the 1570C subjected to ECAE up to true strains of ~ 3 and ~ 8 , respectively.

Table 1. Mechanical properties of the 1570C alloy in initial state and after ECAE

State	YS (0.2%) (MPa)	UTS (MPa)	Elongation (%)
Initial state	238±3	354±6	28±1
ECAE with a total strain of $\varepsilon\sim 3$	309±4	390±2	32±3
ECAE with a total strain of $\varepsilon\sim 8$	300±4	379±6	31±2

As a result, the fracture toughness for the 1570C alloy with fully recrystallized structure attained a value of $43 \pm 2 \text{ MPa}\cdot\sqrt{\text{m}}$, while this value for the alloy with partially recrystallized structure was found to be $33 \pm 2 \text{ MPa}\cdot\sqrt{\text{m}}$. Therefore, the formation of fully recrystallized structure provides achieving higher crack propagation resistance in spite of slightly lower strength.

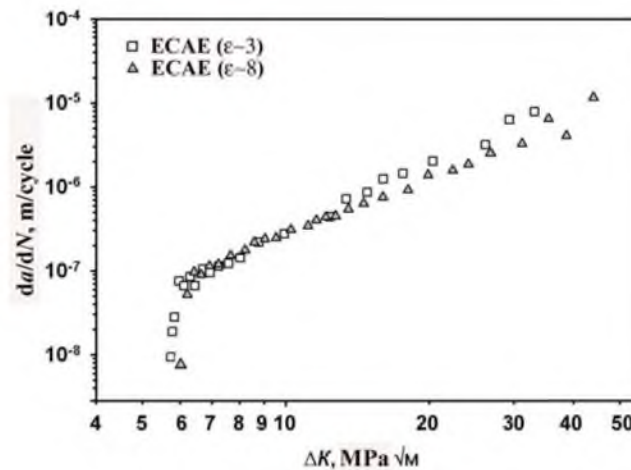


Figure 2. Relationships between crack growth rate and stress intensity factor range.

Crack paths and fractography are represented in Fig.3 and Fig.4, respectively. Notably, no significant difference in fatigue crack growth paths for two states of the 1570C alloy was found at low and moderate values of the stress intensity factor range. However, at larger values ΔK close to $\sim 30 \text{ MPa}\cdot\sqrt{\text{m}}$ (Fig.3), the crack propagation surface for the sample strained up to $\varepsilon\sim 3$ is more smooth (Fig.3a) than that deformed to $\varepsilon\sim 8$; that induces a higher fatigue crack growth rate. Examination of fatigue crack surfaces (Fig.4) supports this conclusion. At high values of stress intensity factor range, ΔK , both samples exhibit coarse fracture surface, where the fracture crack growth seems to occur by classical crack-tip blunting mechanism that gives rise to striations formation accompanied by opening secondary cracks [3]. At the same time, in the samples with partially recrystallized structure many cracks that grow along deformation bands are also observed. These can give an additional contribution in acceleration of fatigue crack growth rate.

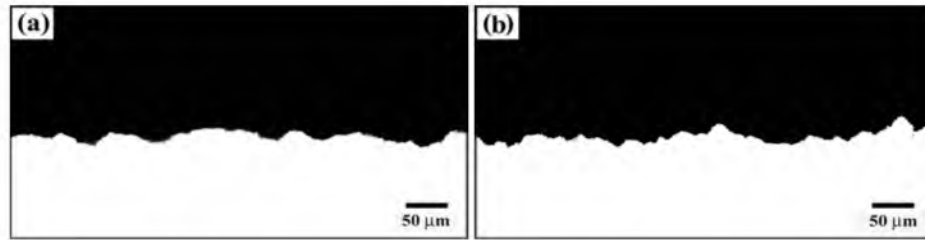


Figure 3. Optical micrographs for fatigue crack growth paths at 13 mm from the straight through notch for the 1570C subjected to ECAE up to a total strain of ~3 (a) and ~8 (b).

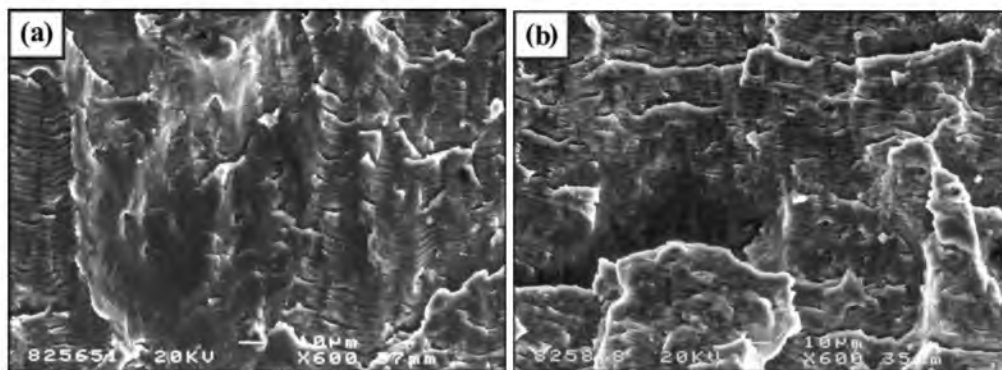


Figure 4. Fatigue crack surfaces at $\Delta K \sim 30 \text{ MPa}\cdot\sqrt{\text{m}}$ for the 1570C subjected to ECAE up to a total strain of ~3 (a) and ~8 (b).

4. Summary

The 1570C alloy belonging to Al-Mg-Sc system was subjected to large strain by ECAE. This processing resulted in fully recrystallized structure with an average grain size of $\sim 1.2 \mu\text{m}$ and enhancement of strength and crack propagation resistance. Values of fatigue crack growth ($da/dN = 3,4 \times 10^{-6} \text{ m/cycle}$ at $\Delta K = 30 \text{ MPa}\cdot\sqrt{\text{m}}$) and fracture toughness ($\Delta K_{\text{max}} = 43 \pm 2 \text{ MPa}\cdot\sqrt{\text{m}}$) are close to these properties of AA2324 alloy that allow considering the 1570C alloy for aircraft applications.

Acknowledgements

This work was supported by the International Science and Technology Center under grant No.2011 and Federal Agency of Education under grant no.P1065 .

References

- [1] Valiev R Z, Islamgaliev R K and Alexandrov I V 2000 *Prog. Mater. Sci.* **45** 103
- [2] Musin F, Kaibyshev R, Motohashi Y and Itoh G 2004 *Scripta Mater.* **50** 511
- [3] Avtokratova E.V., Sitdikov O.Sh., Kaibyshev R.O., Watanabe Y. 2009 *The Physics of Metals and Metallography* 2009 **107** 291
- [4] Avtokratova E.V., Kaibyshev R.O., Sitdikov O.Sh. 2008 *The Physics of Metals and Metallography* **105** 500
- [5] Vinogradov A., Washikita A., Kitagawa k., Kopylov V.I., 2003 *Mater. Sci. Eng.* **349** 318
- [6] Vinogradov A. 2007 *J. Mater. Sci.* **42** 1797
- [7] Kaibyshev R., Avtokratova E, Apollonov A., Davies R. 2006 *Scripta Mater.* **54** 2119